

Weak ductile shear zone beneath the western North Anatolian Fault Zone: inferences from earthquake cycle model constrained by geodetic observations

Tadashi Yamasaki, Tim J. Wright and Gregory A. Houseman
COMET+, School of Earth and Environment, University of Leeds, UK

T23E-2634 Fall AGU 2013



SUMMARY

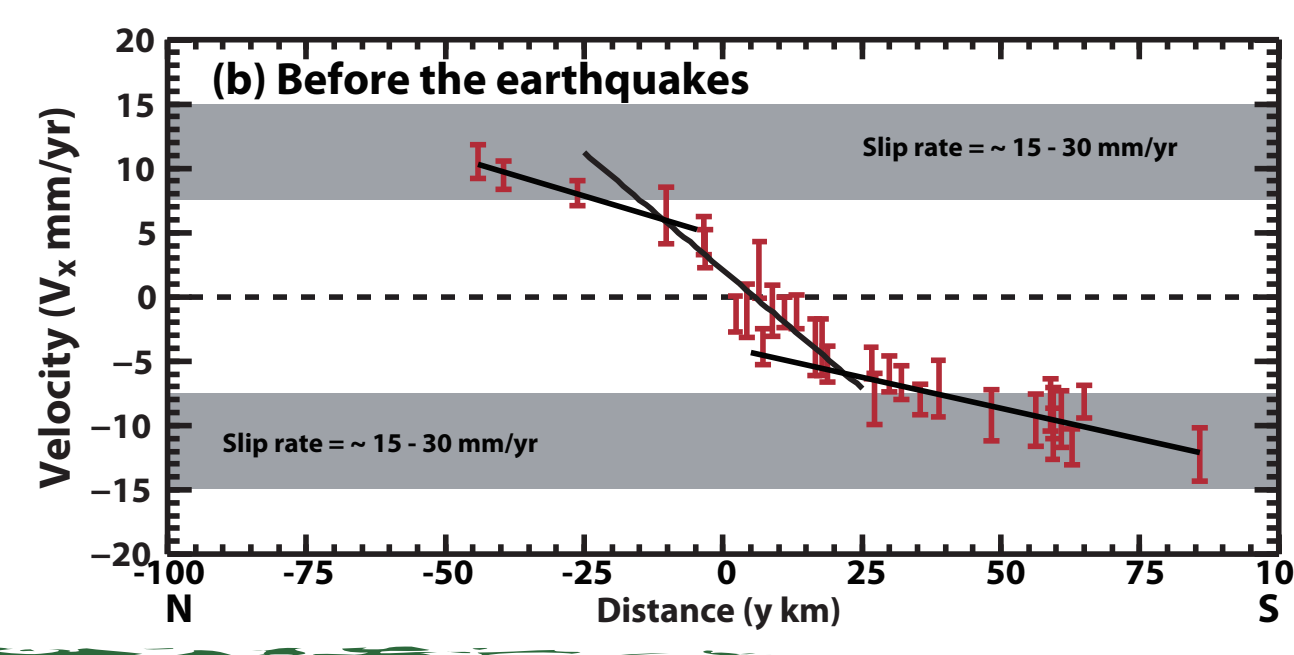
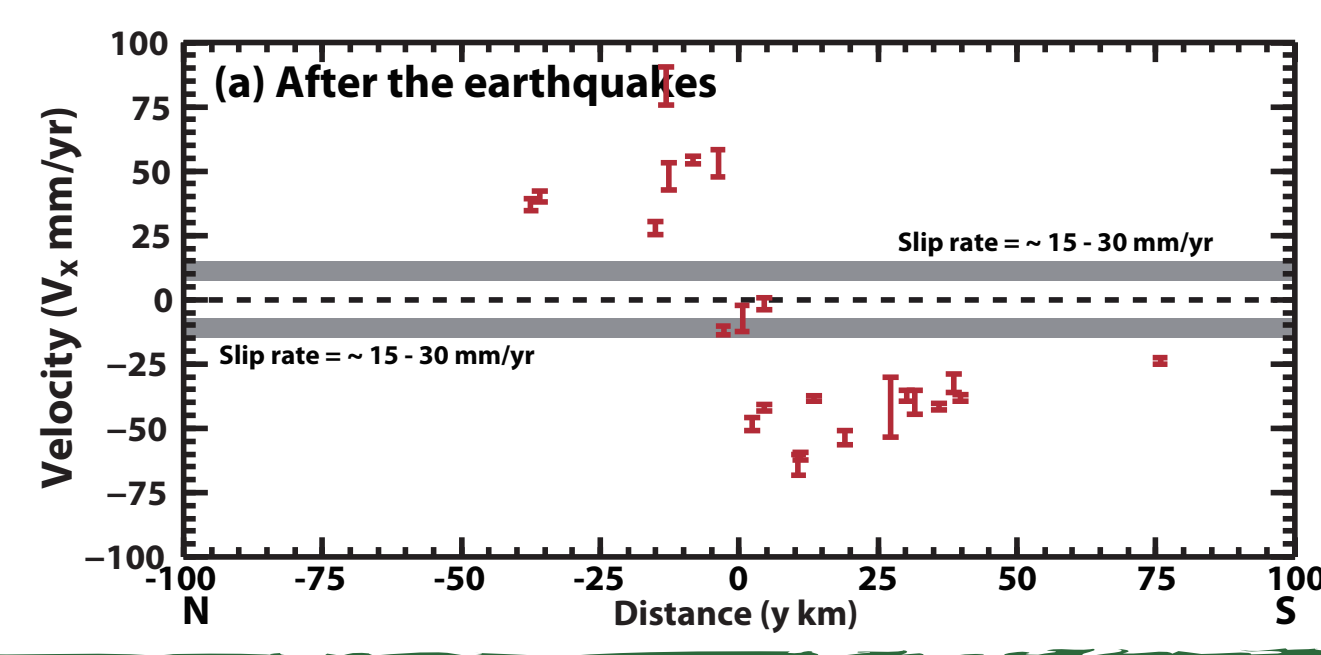
Profiles of GPS velocities across the North Anatolian Fault, before and after the 1999 İzmit and Düzce earthquakes, require a localised weak zone in the mid crust beneath the western North Anatolian Fault Zone. The thickness and width of this low viscosity zone are ~ 12 km and $\sim 20 - 40$ km, respectively, and the effective viscosities of the weakened and the non-weakened domains are $\sim 2 \times 10^{18}$ and $\sim 2 \times 10^{20}$ Pa s, respectively.

1. AIM OF THIS STUDY

Using a 3D finite element model, we examine the linear Maxwell visco-elastic response to a repeated strike-slip faulting event under the condition of a constant far-field loading rate for three basic crustal viscosity models beneath an upper elastic layer: uniform viscosity (UNV), depth-dependent viscosity (DDV) and localised weak zone (LWZ). We compare predicted surface velocity profiles with the GPS velocity profiles across the North Anatolian Fault Zone (NAFZ), before and after the 1999 İzmit and Düzce earthquakes, in order to constrain the actual viscosity variation in the crust.

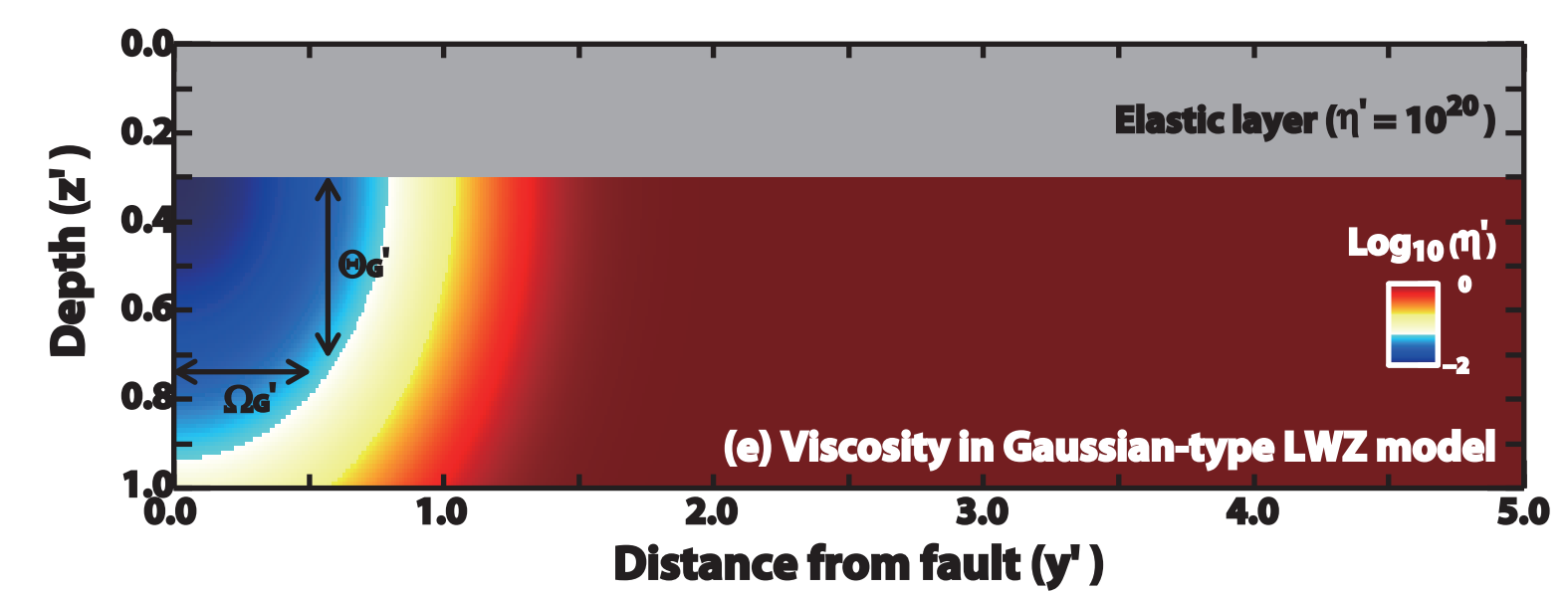
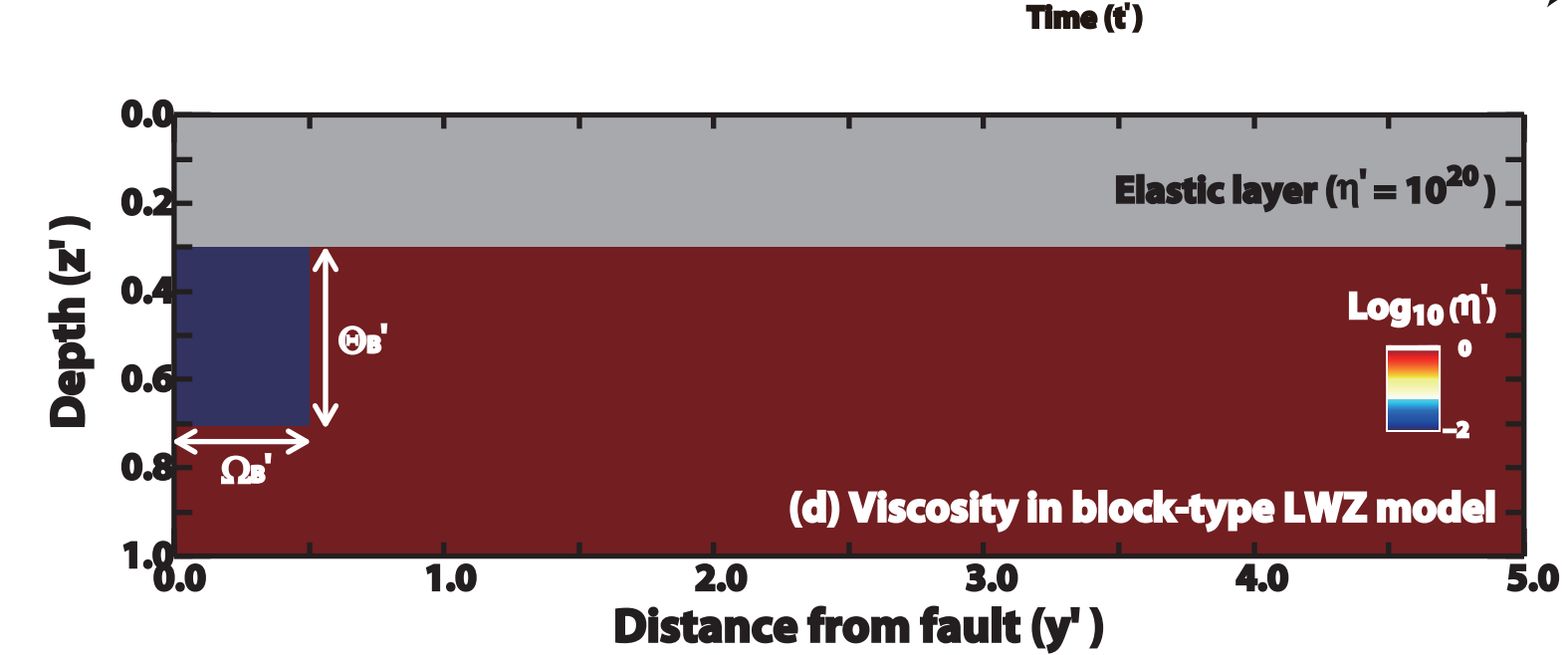
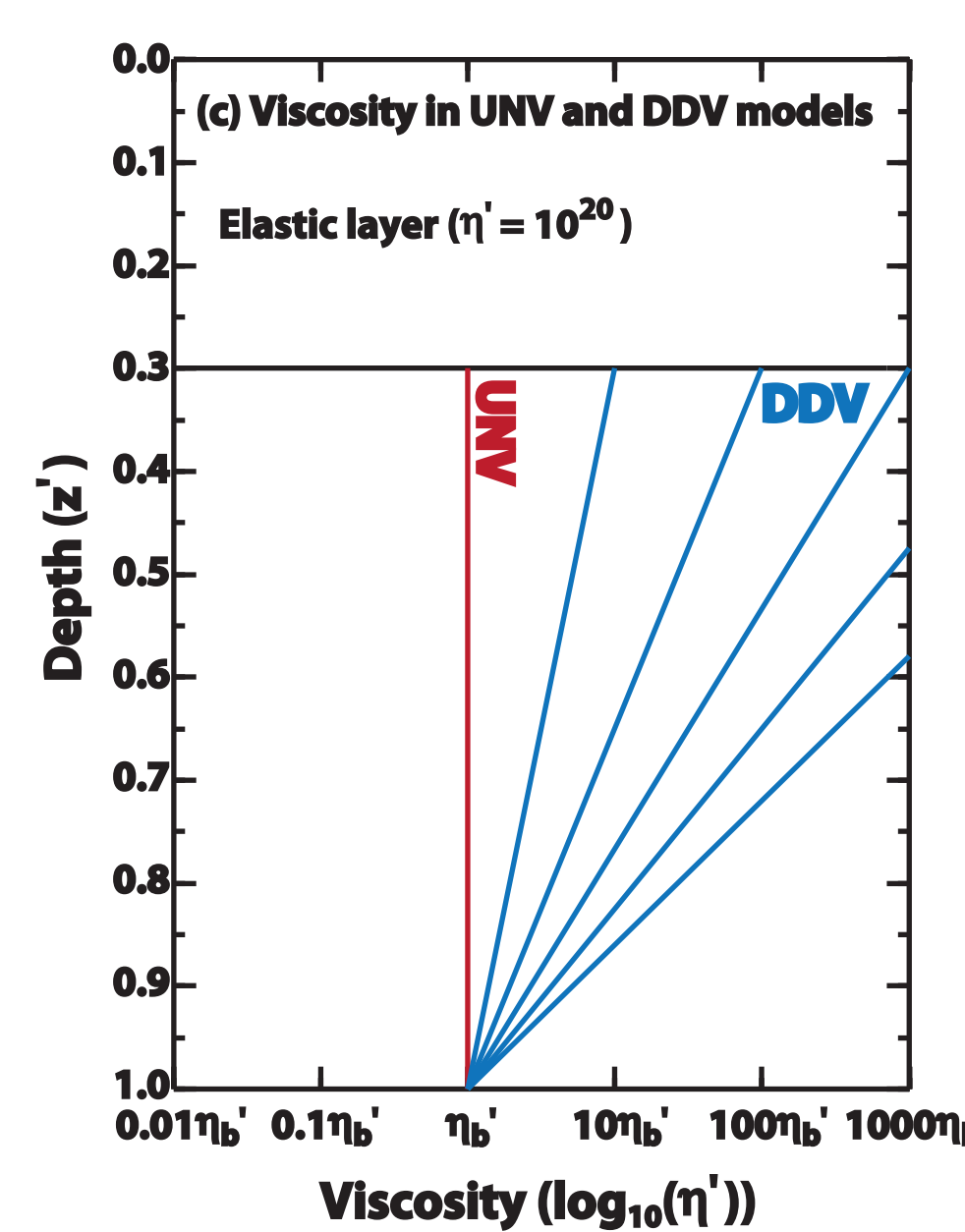
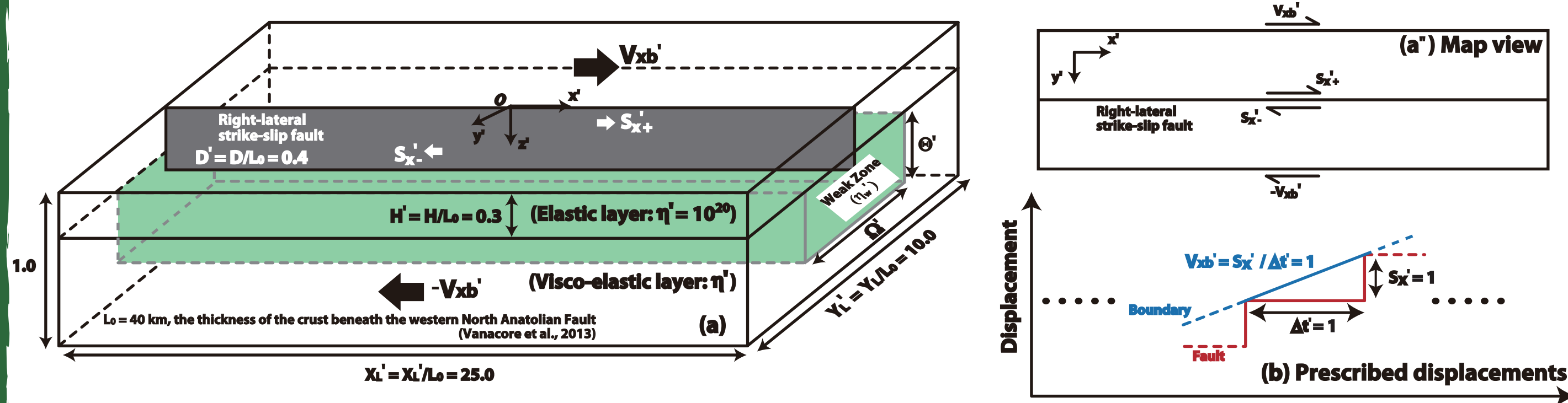
2. THE GEODETIC OBSERVATIONS

The GPS velocity profiles across the North Anatolian Fault Zone near the epicentres of the 1999 İzmit and Düzce earthquakes show: (a) after the earthquakes (Ergintav et al., 2009), the peak velocities either side of the fault differ by as much as 150 mm/yr, 5 or 10 times greater than the long-term relative displacement rate of ~ 15 to 30 mm/yr (Tatar et al., 2012; Reilinger et al., 2006). (b) before the earthquakes (McClusky et al., 2000), displacement rates vary monotonically across fault zone, but the velocity gradient is ~ 3 times higher within a zone of about 30 km width, centred on the fault.



3. THE EARTHQUAKE CYCLE MODEL

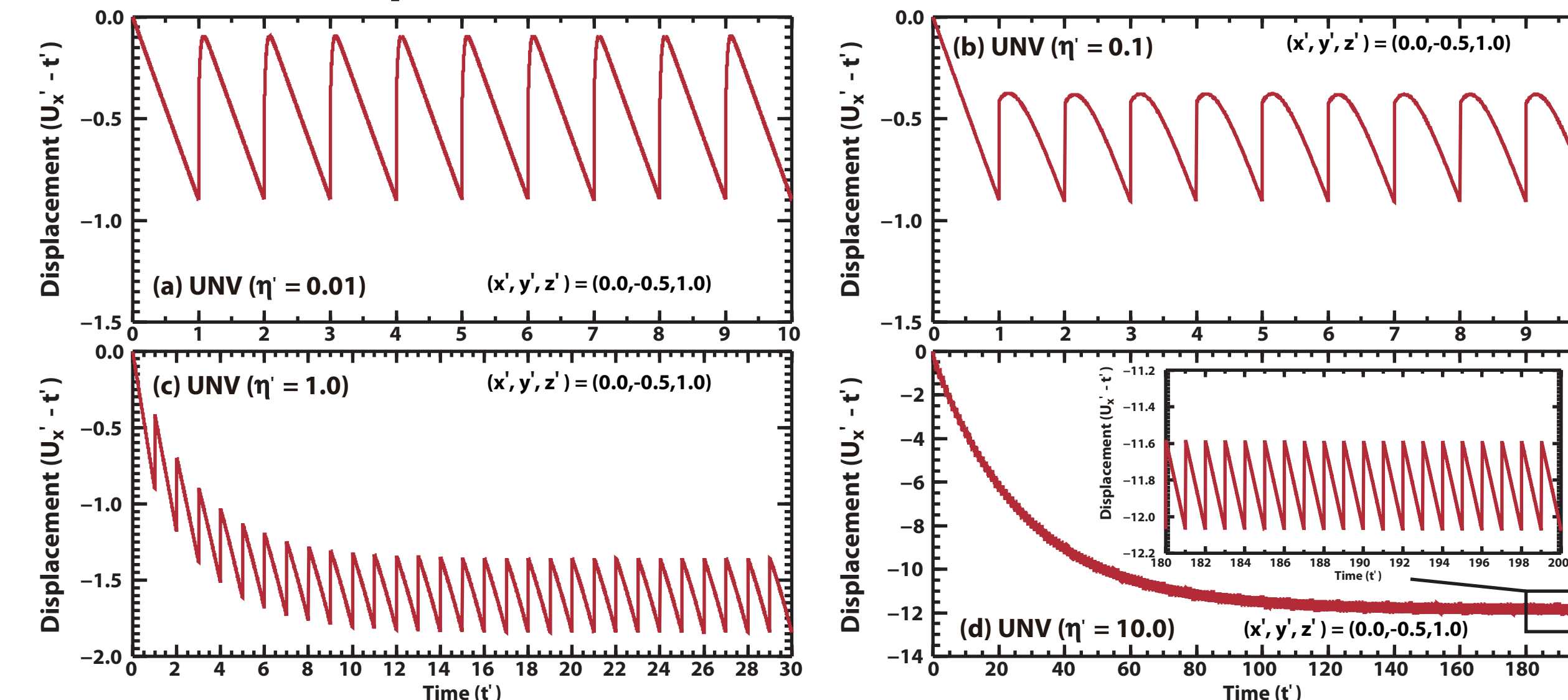
We use a parallelized 3-D finite element code, oregano_ve (Yamasaki and Houseman, 2012), to solve the linear Maxwell visco-elastic problem in which an instantaneous strike-slip fault occurs at a periodic interval, releasing elastic strain accumulated by regional loading that occurs at a constant rate.



4. THE MODEL BEHAVIOUR: INFERENCE FOR THE NAFZ CASE

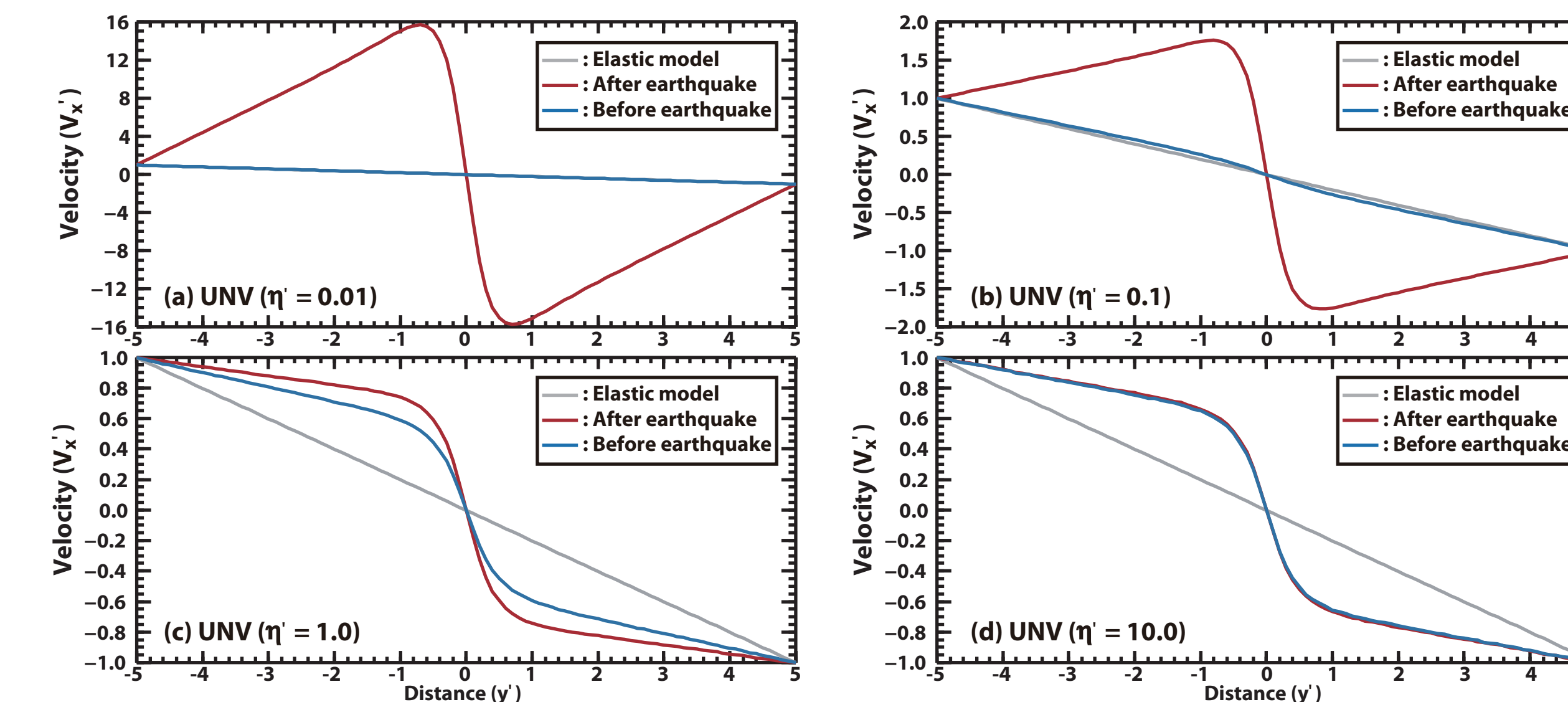
4.1 Uniform viscosity (UNV) model

4.1.1 The surface displacement with time



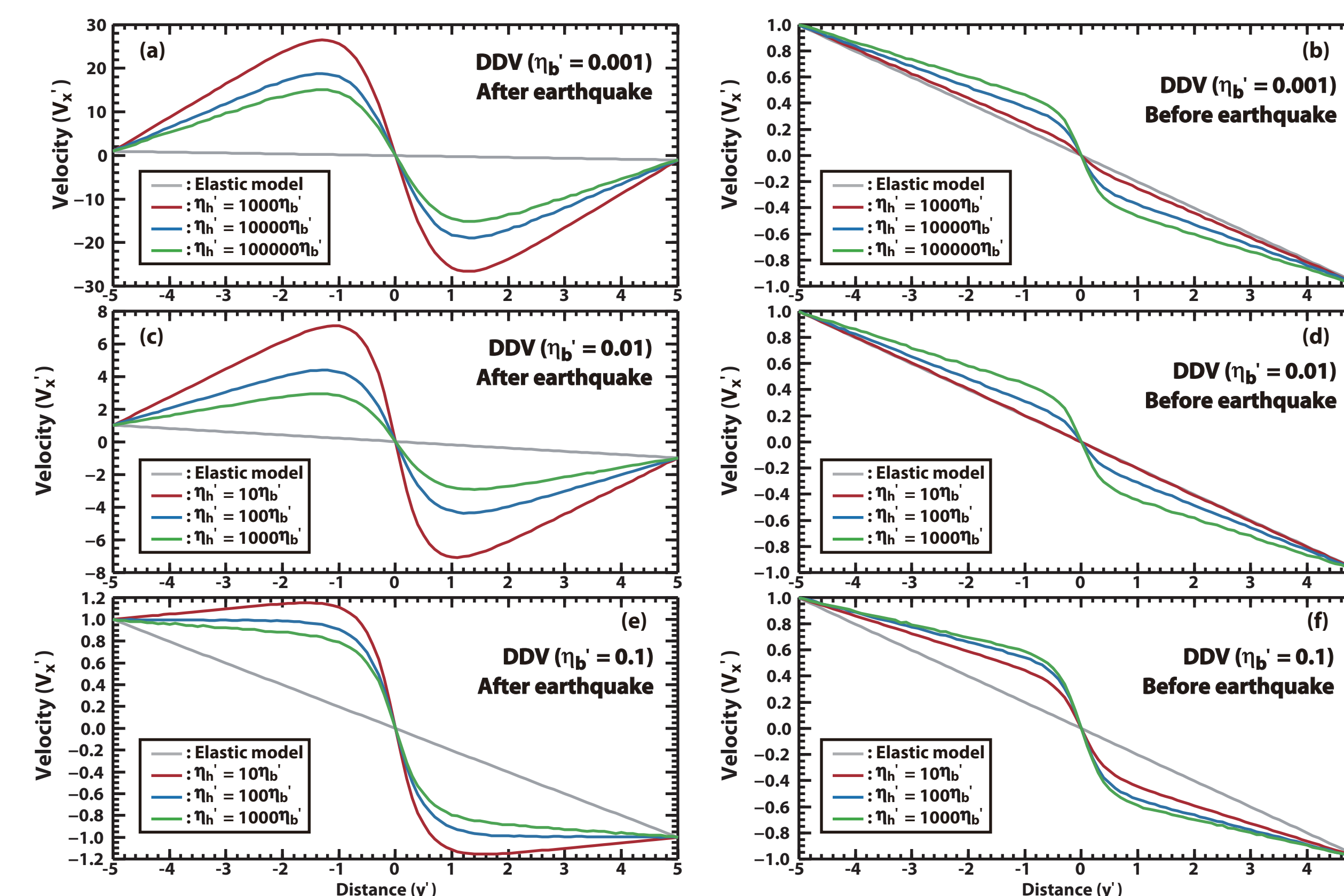
For the models with $\eta' = 0.01$ and 0.1 , a steady-state periodicity is established rapidly, implying that the stress relaxation is virtually completed by the end of the inter-seismic period. For the models with $\eta' = 1.0$ and 10.0 , only a smaller proportion of the deviatoric stress can be relaxed between seismic events, and the un-relaxed stresses evolve until the steady-state is established.

4.1.2 The surface velocity profiles before and after earthquake



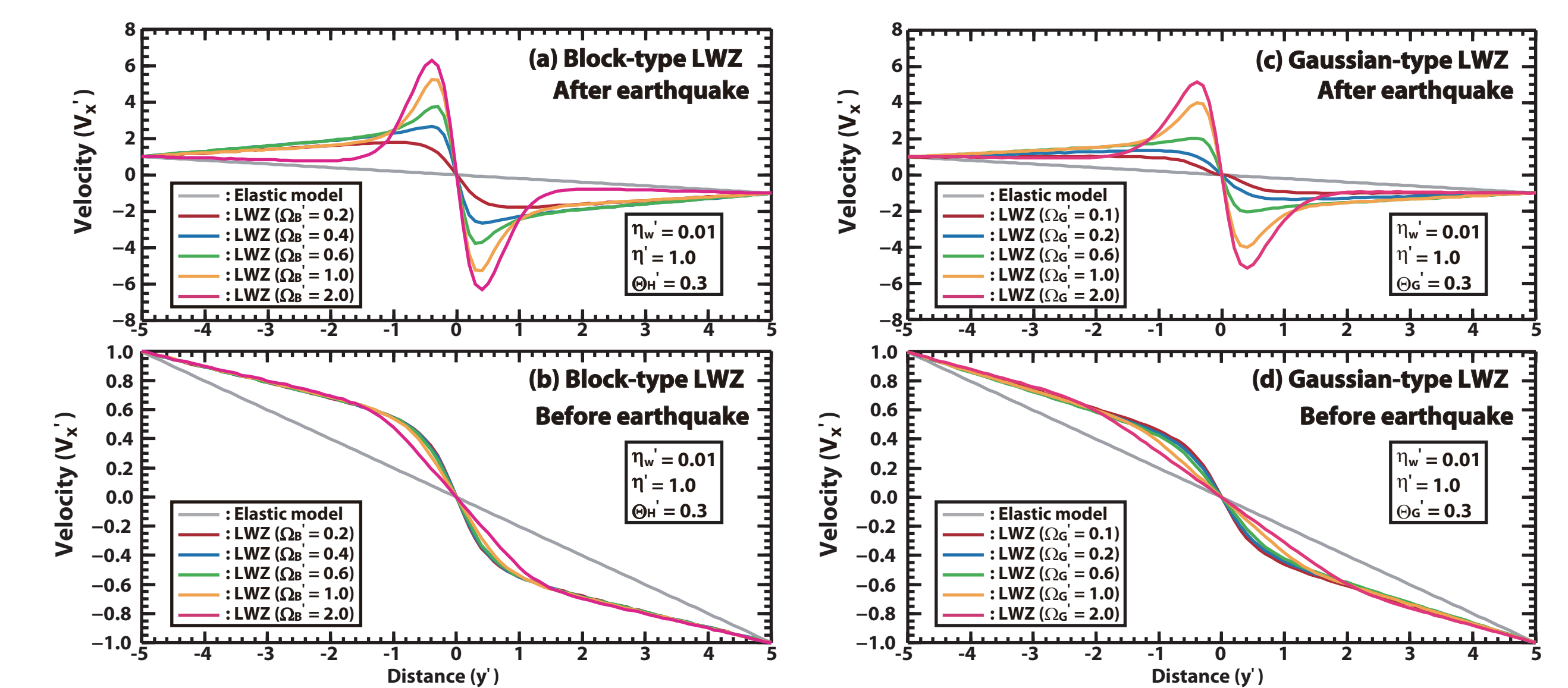
The high post-seismic displacement rate is predicted for UNV model with $\eta' = 0.01$ or 0.1 , but such a model does not predict the higher pre-seismic velocity gradient across the fault. \Rightarrow A UNV model cannot explain the NAFZ velocity profiles.

4.2 Depth-dependent viscosity (DDV) model



Some DDV models predict the general observed features. However, the pre-seismic velocity gradient across the fault is not adequately high, and the wavelength of the post-seismic velocity profile is inconsistent with the data. \Rightarrow A DDV model alone cannot explain the NAFZ velocity profiles.

4.3 Localised weak zone (LWZ) model



LWZ model predicts the general observed features of the both post- and pre-seismic velocities with consistent wavelength of the profiles. Note that the Gaussian-function type of LWZ results in similar behaviour. \Rightarrow An LWZ model can explain the NAFZ velocity profiles.

5. THE LWZ MODEL FOR THE NAFZ CASE

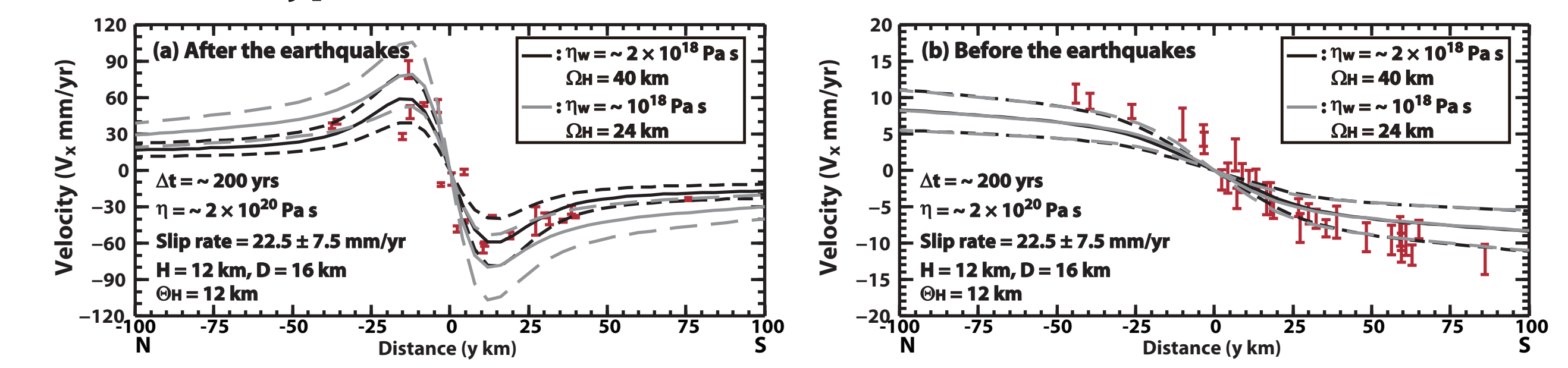
The LWZ model prediction shows a good fit to both pre- and post-seismic data for the LWZ configuration shown in Table 1.

Asymmetry of the observed profiles is not included in these LWZ models.

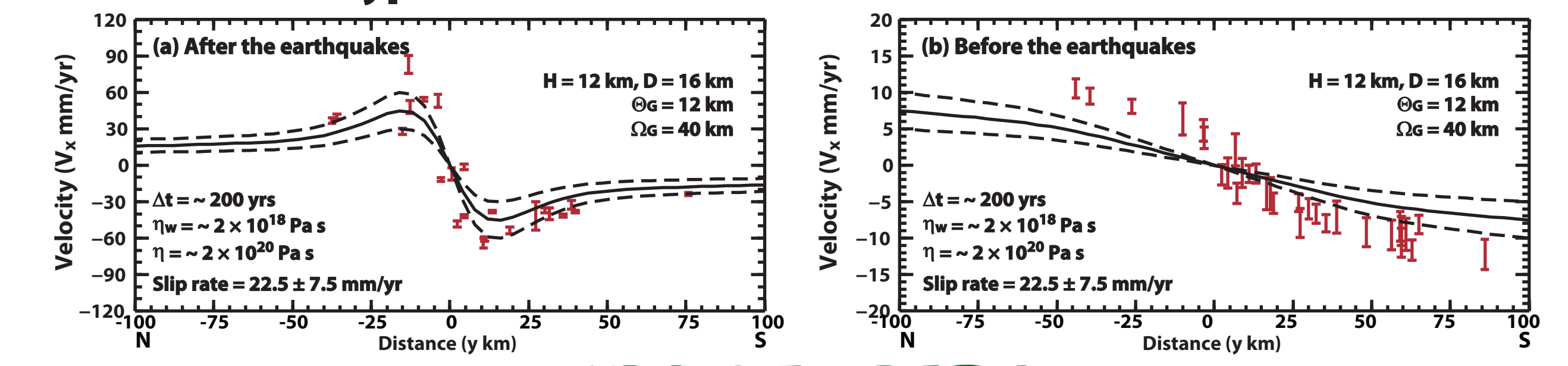
Comparison with observations favours the block-type LWZ rather than the Gaussian-type LWZ.

Symbol	Meaning	Value
L_0	Layer thickness	40 km
μ	Shear modulus	3×10^{10} Pa
ν	Poisson's ratio	0.25
H	Elastic layer thickness	12 km
D	Depth-averaged of fault	16 km
Δt	Earthquake cycle period	~ 200 yrs
η	Background viscosity	$\sim 2 \times 10^{20}$ Pa s
η'	Minimum viscosity in localised weak zone (LWZ)	$\sim 2 \times 10^{18}$ Pa s
Ω_H, Ω_D	(Effective) width of LWZ	$\sim 24 - 40$ km
Θ_H, Θ_D	(Effective) thickness of LWZ	~ 12 km
$2S_0/\Delta t$	Slip rate	$\sim 15 - 30$ mm/yr
V_{00}	Boundary velocity	$\sim 7.5 - 15$ mm/yr

5.1 The Block-type of LWZ



5.2 The Gaussian-type of LWZ



6. CONCLUSIONS

- (1) The ratio $\tau/\Delta t$ of the Maxwell relaxation time τ to the earthquake cycle period Δt controls the surface velocity variation during the earthquake cycle.
- (2) Post-seismic velocities near a major fault that are much greater than the long-term relative displacement rate indicate a relatively low Maxwell time near constant (low viscosities), and strong localization of the pre-seismic strain rate near the fault requires a relatively high Maxwell time constant (high viscosities).
- (3) Of the models we tested, only the localized weak zone (LWZ) model is able to explain at once the GPS velocities before and after the 1999 İzmit and Düzce earthquakes. We infer a zone of low viscosity ($\sim 2 \times 10^{18}$ Pa s) centred below the fault, relative to a general background crustal viscosity of at least 2×10^{20} Pa s. The low viscosity zone is ~ 12 km thick (below a 12 km thick elastic layer), and its width is between ~ 20 and 40 km.
- (4) A likely explanation for the block-type low viscosity zone is a slice of allocthonous crust about 20 km wide between northern and southern strands of the North Anatolian Fault in the İzmit region, though differences in stress, grain-size, water content, or temperature could also be significant.

ACKNOWLEDGEMENTS:

This study is supported by the UK Natural Environment Research Council (NERC) under grant number NE/I028017/1, and with the support of the National Centre for Earth Observation (NCEO-COMET+). Cluster computing was provided by NCEO and by the University of Leeds Advanced Research Computing Node 1 (arc1).

REFERENCES:

Bürgmann et al., 2002, BSSA 92, 126-137; Ergintav et al. 2009, JGR 114, B07403, doi:10.1029/2008JB006021; Feigl et al., 2002, BSSA 92, 138-160; Klinger et al., 2003, BSSA 93, 2317-2332; Kozaci et al., 2009, JGR 114, B01405, doi:10.1029/2008JB005760; McClusky et al., 2000, JGR 105, 5695-5719; Reilinger et al., 2000, Science 289, 1519-1524; Reilinger et al., 2006, JGR 111, B05411, doi:10.1029/2005JB004051; Rockwell et al., 2009, Geol. Soc. Lon. Spec. Pub. 316, 31-54; Stein et al., 1997, GJI 128, 594-604; Vanacore et al., 2013, GJI, 193, 329-337; Tatar et al., 2012, Tectonophysics 518-521, 55-62; Wright et al., 2001, GRL 28, 2117-2120; Yamasaki & Houseman, 2012, GJI 190, 769-784.